Barrier inhomogeneity and electrical properties of Pt/GaN Schottky contacts

Ferdinando Iucolano[a)]
Istituto per la Microelettronica e Microsistemi (CNR-IMM), Consiglio Nazionale delle Ricerche, Stradale Primosole 50, 95121 Catania, Italy and Dipartimento di Fisica ed Astronomia, Università di Catania, Via S. Sofia 64, 95121 Catania, Italy

Fabrizio Roccaforte, Filippo Giannazzo, and Vito Raineri
Istituto per la Microelettronica e Microsistemi (CNR-IMM), Consiglio Nazionale delle Ricerche, Stradale Primosole 50, 95121 Catania, Italy

(Received 31 July 2007; accepted 1 October 2007; published online 3 December 2007)

The temperature dependence of the electrical properties of Pt/GaN Schottky barrier was studied. In particular, a Schottky barrier height of 0.96 eV and an ideality factor of 1.16 were found after a postdeposition annealing at 400 °C. Nanoscale electrical characterization was carried out by the conductive biased tip of an atomic force microscope both on the bare GaN surface and on the Pt/GaN contacts. The presence of a lateral inhomogeneity of the Schottky barrier, with a Gaussian distribution of the barrier height values, was demonstrated. Moreover, GaN surface defects were demonstrated to act as local preferential paths for the current conduction. The temperature dependent electrical characteristics of the diodes were discussed in terms of the existing models on inhomogeneous barriers and correlated to the nanoscale electrical characterization of the barrier. In this way, the anomalous electrical behavior of the ideality factor and of the Schottky barrier and the low experimental value of the Richardson's constant were explained. © *2007 American Institute of Physics*. [DOI: 10.1063/1.2817647]

I. INTRODUCTION

For a few years, gallium nitride (GaN) has been exploited for the fabrication of high efficiency optoelectronics devices, such as light emitting diodes and laser.[1] Moreover, its outstanding properties (wide band gap, high critical electric field, and high electron saturation velocity), make it a promising material for high-power and high-frequency devices applications.[2] However, to date, the lack of high quality freestanding GaN substrates, as well as the high dislocations density of the heteroepitaxial layers, has limited the development of reliable large area high-power devices.[3]

Schottky contacts are fundamental units of both high-power GaN rectifiers and high electron mobility transistors. Nevertheless, obtaining reproducible rectifying contacts on GaN with a high and ideal Schottky barrier Φ_B and a low leakage current still remains a serious technological concern, whose physical origin is continuously object of investigation. Typically, metals with a high work function (such as Pt, Ni, and Pd) are used for Schottky contacts to *n*-type GaN since, according to the Schottky-Mott relation,[4] they are expected to give high Schottky barrier height values. However, several authors have found low experimental values of Φ_B and ideality factors *n* significantly larger than the unity.[5–7] The wide range of variability of the barrier heights, particularly in no-nannealed contacts, is sometimes ascribed to a partial Fermi level pinning at the metal/GaN interface in the presence of a large density of surface states.[8–10] Obviously, low values of the barrier height result into a high reverse leakage current, which is, in turn, detrimental for the device performances. Another commonly observed anomaly in GaN, similarly to other semiconductors such as GaAs and SiC,[11,12] is that the experimental values of the Richardson's constant A^* may be significantly lower (even orders of magnitude) than the theoretical value of 26.9 A cm^{-2} K^{-2}.[13–15] These discrepancies are still a scientific open issue, and they were attributed to different factors, such as the enhanced tunneling current through the metal/GaN Schottky barrier or to the presence of charged surface states, metal induced gap states, chemical reactions at the interface, bulk material defects, etc. Consequently, systematic studies on the electrical behavior of Schottky contacts on GaN are always important to acquire a deeper knowledge of the electrical parameters (barrier height, ideality factor, and Richardson's constant) and of the current transport mechanisms and to understand how these parameters and the device performances are influenced by the continuous evolution of the material quality.

In this context, the improvement of the nanoscale characterization techniques to monitor the metal/GaN interfacial properties allowed significant progresses in the comprehension of the electrical behavior of macroscopic GaN-based devices.[16–18] In particular, we have recently demonstrated a correlation between the nanoscale electrical properties of the Pt/GaN barrier, monitored by means of conductive atomic force microscopy (C-AFM), and the experimental temperature behavior of macroscopic Schottky contacts.[19]

In this work, a detailed analysis of the temperature dependence of the characteristics of Pt/GaN Schottky contacts has been carried out to clarify the origin of the anomalous behavior of the barrier height and of the ideality factor and the significant underestimation of the Richardson's constant. A nanoscale electrical characterization demonstrated the formation of an inhomogeneous Schottky barrier. The results

[a)]Electronic mail: ferdinando.iucolano@imm.cnr.it

were discussed in terms of the models considering the barrier inhomogeneity. Furthermore, the material quality was indicated as one of the possible physical causes of the experimentally observed electrical behavior of the Pt/GaN barrier.

II. EXPERIMENTAL

Silicon doped n-type ($N_D \sim 1\times10^{16}$ cm^{-3}) GaN epitaxial layers, 3 μm thick, on a heavily doped n^+ GaN buffer layer, grown on sapphire substrates supplied by Lumilog, were used. Circular Schottky diodes were fabricated in order to study the macroscopic electrical characteristics of the contacts as a function of temperature. A Ti/Al/Ni/Au multilayer was sputtered and subsequently annealed at 750 °C in Ar (Ref. 20) to form a large area ring-shaped Ohmic contact. The Schottky contact (of area 7.1×10^{-4} cm^2) was formed by the deposition of a $Pt_{(80\ nm)}/Au_{(120\ nm)}$ bilayer and defined by optical lithography and lift-off processes. Postdeposition isochronal rapid annealing processes for 60 s in the range of 300–500 °C were performed in Ar atmosphere using a Jetfirst Jipelec rapid furnace.

The current-voltage (I-V) characteristics of the Schottky diodes were measured at different temperatures, ranging between 25 and 175 °C, using a temperature controlled Suss Microtec probe station equipped with an Agilent 4155C parameter analyzer.

In order to study the nanoscale electrical properties of the Schottky barrier, local I-V measurements were performed on the Pt/GaN sample using a DI-3100 atomic force microscope (AFM) with Nanoscope V controller by Veeco with a biased conductive diamond-coated Si tip.[21] The sample preparation for these measurements is described in detail in Ref. 19. Moreover, scanning capacitance microscopy (SCM) analysis was also carried out on the bare GaN surface to have information both on the type of the local doping and on the carrier concentration.

III. RESULTS AND DISCUSSION

A. Temperature dependence of the Pt/GaN Schottky barrier electrical characteristics

First, the electrical forward I-V measurements were performed on several Au/Pt/GaN Schottky diodes, before and after postdeposition annealing processes between 300 and 500 °C. After annealing, significant changes of the electrical characteristics could be observed with respect to the as-deposited sample. The optimization of the characteristics, in terms of barrier height and ideality factor, was achieved after an annealing at a temperature of 400 °C. Hence, in Fig. 1, we report in a semilogarithmic scale a forward I-V characteristic, representative of the on average behavior of the devices annealed at 400 °C, compared with the I-V curves of the as-deposited sample. Clearly, after annealing, a shift of the I-V curves toward higher biases and an improvement of the linearity are observed.

The Schottky barrier height Φ_B and the ideality factor n were determined from a fit of the linear region of the forward I-V curves, where $qV > 3kT$, using the following thermionic emission model:[4]

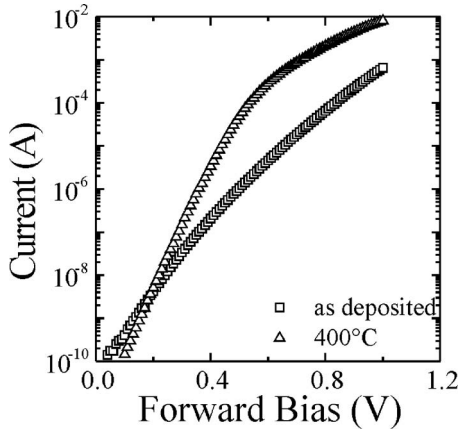

FIG. 1. Forward I-V characteristics of the Au/Pt/GaN Schottky diodes before and after an annealing at 400 °C.

$$I = AA^*T^2 \exp\left(-\frac{q\Phi_B}{kT}\right)\exp\left(\frac{qV}{nkT}\right) = I_S \exp\left(\frac{qV}{nkT}\right), \quad (1)$$

where A is the contact area, A^* is the Richardson constant, T is the absolute temperature, q is the electron charge, k is the Boltzmann constant, Φ_B is the Schottky barrier height, and n is the ideality factor. For this calculation, the theoretical value of the Richardson's constant for GaN (A^* = 26.9 A cm^{-2} K^{-2}) (Ref. 22) was used. The saturation current I_s can be extrapolated at $V=0$ from the linear fit of the forward I-V curves.

For the as-deposited contact, a Schottky barrier height Φ_B=0.79 eV and an ideality factor of n=1.80 were found. On the other hand, after annealing of the contact at 400 °C, an increase of the barrier height from 0.79 to 0.96 eV is observed, accompanied by a significant improvement of the ideality factor n from 1.80 to 1.16.

Other authors reported an improvement of the electrical characteristics of Schottky contacts on GaN by postdeposition rapid thermal annealing at similar temperatures.[5–7] However, an electrical degradation of the contacts may occur when performing annealing at higher temperatures and/or for longer times.[23,24]

In order to get further insights in the carrier transport through the metal/GaN contact and on the electrical parameters, the forward current-voltage characteristics were measured at several temperatures (I-V-T). As an example, it is here reported for the sample annealed at 400 °C, i.e., the annealing temperature at which the diodes exhibited an improved ideality factor (n=1.16) at room temperature. Figure 2 shows the forward I-V characteristics as a function of temperature for the annealed Pt/GaN diodes. As predicted by the thermionic emission model, the forward current of the diodes at a fixed bias increases with increasing the temperature. From these I-V-T curves, the values of the Schottky barrier height Φ_B and of the ideality factor n of the diodes were determined and are reported in Fig. 3(a) as a function of the temperature. A dependence of both Φ_B and n on the temperature is clearly observed. In particular, the barrier height increases, while the ideality factor decreases with increasing the measurement temperature. Such a temperature behavior both of the barrier height and of the ideality factor is com-

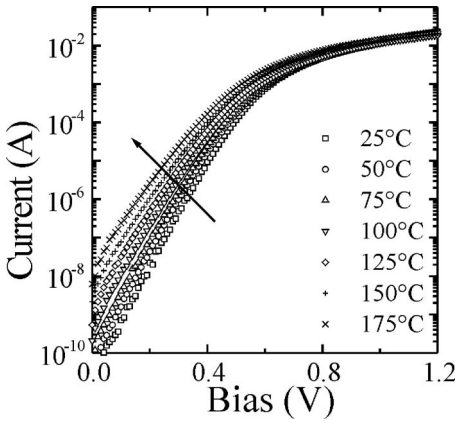

FIG. 2. Forward *I-V* characteristics of the Au/Pt/GaN Schottky diodes at increasing temperatures (in the arrow direction) in the range of 25–175 °C, for the sample annealed at 400 °C.

monly observed in "real" Schottky barriers and attributed to the inhomogeneity of the contact. Figure 3(b) reports the values of the Schottky barrier Φ_B as a function of the ideality factor. An almost linear correlation between Φ_B and n can be observed. According to Schmitsdorf *et al.*[25] and Tung,[26] this behavior can be associated with the presence of a "nonuniform" Schottky contact.

From the experimental data reported in Fig. 2, the values of the saturation current I_S were determined at each temperature, and a "conventional" Richardson's plot, $\ln(I_S/T^2)$ versus $1/kT$, is reported in Fig. 4. When trying to fit the experimental data, a deviation from linearity is clearly visible at the low temperatures. From this fit, a Schottky barrier height

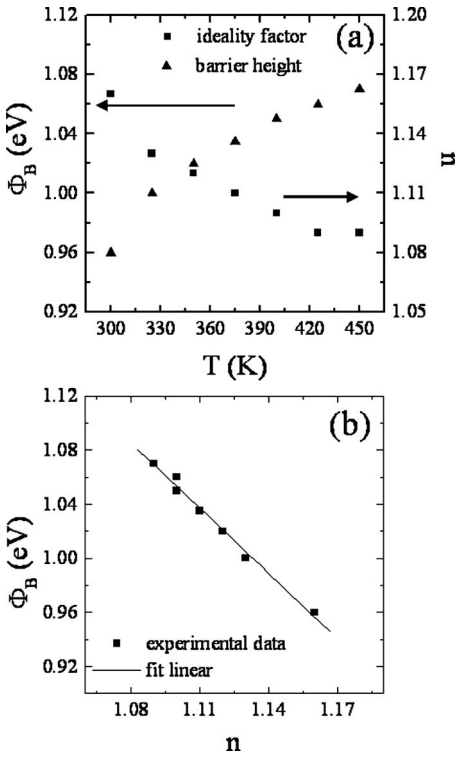

FIG. 3. (a) Schottky barrier height Φ_B and ideality factor n, determined from the data in Fig. 2(a), as a function of the temperature. Plot of Φ_B vs n showing a linear correlation between these parameters; the extrapolation at $n=1$ gives a value of the ideal barrier $\Phi_{B0}=1.21$ eV.

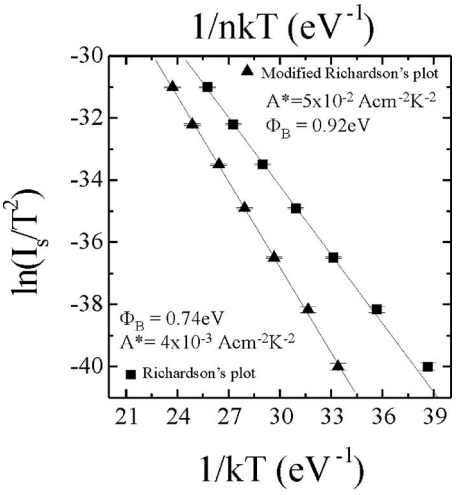

FIG. 4. "Conventional" Richardson plot $\ln(I_s/T^2)$ vs $1/k_BT$ and "modified" Richardson's plot $\ln(I_s/T^2)$ vs $1/nk_BT$ for the sample annealed at 400 °C.

$\Phi_B=0.74$ eV and the Richardson's constant $A^*=4\times10^{-3}$ A cm^{-2} K^{-2} were extracted, this latter being almost four orders of magnitude lower than the theoretical value of A^* for GaN (26.9 A cm^{-2} K^{-2}). The conventional Richardson's plot, however, is based on the thermionic emission mechanism [Eq. (1)] and, hence, assumes an almost ideal barrier, with the ideality factor and the Schottky barrier height independent of the temperature. Hence, the nonlinearity of the conventional Richardson's plot can be associated with the previously shown experimental evidences, namely, the temperature dependence of Φ_B and n. In order to take into account the deviation from the ideality and the experimentally observed dependence of n and Φ_B on the temperature, a "modified" Richardson's plot, $\ln(I_S/T^2)$ versus $1/nkT$, is also reported in Fig. 4. This approach was proposed by Hackam and Harrop[27] in order to consider the effects of deviation from $n=1$ at zero bias voltage as well. In this case, the linear behavior fits better the experimental data also at the lowest temperatures, giving a barrier height value of 0.92 eV and a Richardson's constant of 5×10^{-2} A cm^{-2} K^{-2}. This value of A^*, however, is still significantly lower than the theoretical predictions (26.9 A cm^{-2} K^{-2}). Zhou *et al.*[28] found that the value of A^* determined by a modified Richardson's plot in freestanding GaN material is close to the theoretical value. On the other hand, Ishikawa *et al.*[29] found a reasonable value of Richardson's constant A^* through a conventional Richardson's plot. Clearly, the wide range of variability of these results can be ascribed to the different interface quality, which, in turn, depends on several factors such as the surface defects density, the surface treatment (cleaning, etching, etc.), the metal and the deposition process (evaporation, sputtering, etc.), etc. As an example, Arehart *et al.*[30] observed a dependence of A^* on the dislocation density of the material, in Ni/GaN Schottky diodes. In our case, it can be argued that the underestimation of the A^* value, even after considering the nonideality of the barrier in the Richardson's plot, can be related to the formation of a laterally inhomogeneous Schottky barrier which, in turn, may result into an effective area for the current conduction lower than the total area of the diode. This latter is

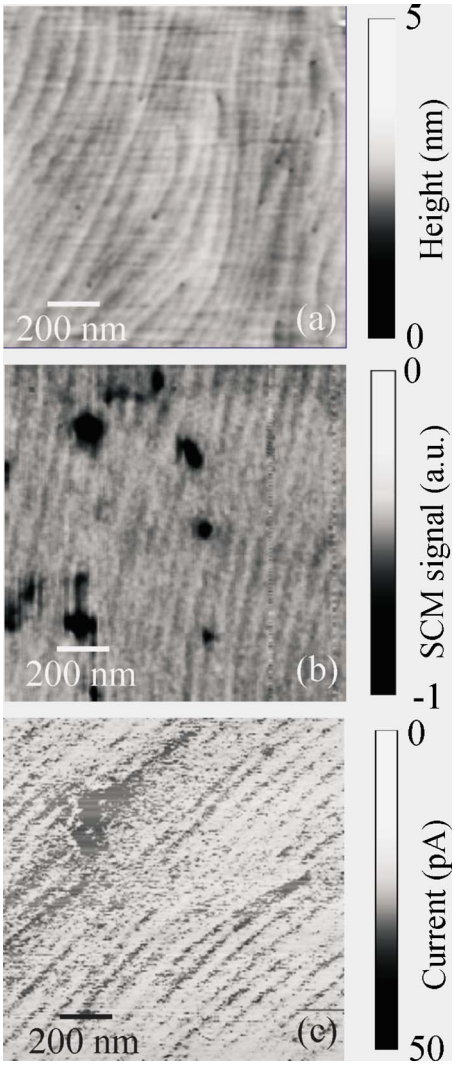

FIG. 5. (a) AFM morphological image (tapping mode), (b) SCM map, and (c) CAFM map on the bare GaN surface.

discussed in more detail in the next section, where a nanoscale characterization of the metal/GaN interface is presented. The same behavior was observed for the as-deposited sample.

B. Nanoscale analysis of the barrier height distribution

Although the above results are consistent with the formation of a laterally inhomogeneous barrier, the conventional electrical analysis of the macroscopic diodes is not exhaustive to reveal the microscopic nature of the barrier inhomogeneity. In this sense, only a combination between the macroscopic *I-V* measurements and a nanoscale local electrical characterization can provide a complete description of the Schottky barrier and fully explain the anomalous temperature dependent electrical parameters.

Since the macroscopic electrical behavior of Pt/GaN Schottky diodes could depend both on the GaN material quality and on the metal/semiconductor interfacial properties, an accurate nanoscale electrical characterization both on the bare GaN surface and on the GaN epilayer coated by a thin Pt/Au film was carried out. In Fig. 5(a), the morphology of the GaN epilayer surface, obtained by tapping mode AFM on a 1.5×1.5 μm^2, is reported. Epitaxial steps on the surface are clearly evidenced. Moreover, peculiar structural defects represented by small holes (10–20 nm diameters) located at the crossing of epitaxial steps are also present, which can be associated with the threading dislocations reaching the surface. From morphological images, their density can be estimated in the order of $\sim5\times10^8$ cm^{-2}. In order to investigate the impact of structural defects on the surface local electronic properties of the GaN material, two different nanoscale electrical characterization techniques based on contact mode AFM have been used, i.e., scanning capacitance microscopy (SCM) and conductive atomic force microscopy (C-AFM). In Fig. 5(b), the SCM map on the GaN surface on a 1.5×1.5 μm^2 area is reported. SCM measures the local capacitance variations (dC/dV) of the nanometric metal-insulator-semiconductor system formed by the conductive AFM tip, the native oxide, and the GaN, in response to a high-frequency (100 kHz) modulating ac bias.[31] In our samples, 0 V dc bias and 0.5 V ac bias were applied between a macroscopic Ohmic contact on the sample surface and the conductive tip. The SCM signal gives information both on the local majority carrier concentration and on the doping type. The map in Fig. 5(b) exhibits a set of black spots (dimensions ranging from 50 to 150 nm) on a background striped pattern resembling the pattern of the epitaxial steps in the morphological image [Fig. 5(a)]. The position of the black spots with respect to that background pattern indicates that those spots can be associated with the threading dislocations. Interestingly, the sign and amplitude of the SCM signal in those spots indicate an electron concentration higher than the uniform n^--type GaN concentration. In agreement with Ref. 32, we found that the regions surrounding the core of threading dislocations behave as n^+-type doped regions, whose dimensions are several times larger than the structural dimensions of the defect. In Fig. 5(c), we report the C-AFM map on the bare GaN surface, obtained applying a 2 V dc bias to the conductive diamond-coated tip. Due to the low *n*-type doping ($N_D\sim1\times10^{16}$ cm^{-3}) in the epilayer, the tip/GaN contact can be described as a nanometric metal/semiconductor Schottky contact. Interestingly, the current pattern on the GaN surface is not uniform. Besides a background low current pattern resembling the epitaxial steps, some characteristic higher current spots are evident on the surface. Those spots can be associated with the threading dislocations. Since SCM measurements indicated a n^+ doping in the region surrounding the threading dislocations core, the measured higher current values could be ascribed to a thinner Schottky barrier and then to the onset of thermoionic-tunnel or tunnel current transport mechanisms. Hence, the nanoscale electrical analysis on the bare GaN surface demonstrated an inhomogeneous conductivity pattern, characterized by the presence of preferential conductive paths in the proximity of the surface defects. Similarly, Miller *et al.*[16] demonstrated that threading dislocations are highly localized leakage current paths, which can be dominant source of leakage current, while Brazel *et al.*[17] indicated the dislocations as responsible for a local lowering of the Schottky barrier height. Only Arehart *et al.*[30] recently argued that a high po-

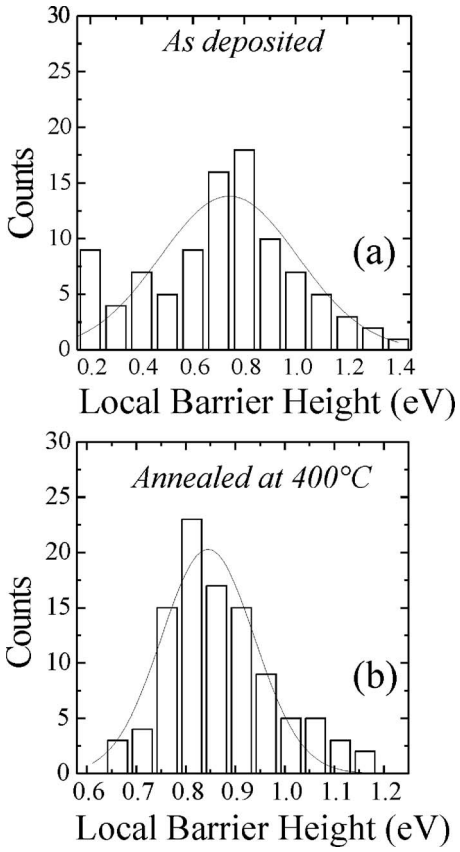

FIG. 6. Statistical distribution of the local barrier height values of the Au/Pt/GaN contact (a) as deposited and (b) annealed at 400 °C. The relative Gaussian fit curve is also reported.

tential barrier in the region surrounding the dislocations is responsible for a localized current blocking in the proximity of the defects, thus leading to a higher barrier to the current flow.

It is important to point out that the morphological and the electrical properties of the GaN surface were not significantly affected by a thermal annealing at 400 °C.

Besides the characterization of the bare GaN surface, in order to have further information on the degree of uniformity of the metal/GaN Schottky barrier, nanoscale local *I-V* measurements were carried out using the biased conductive AFM tip, both on the as-deposited and on the 400 °C annealed Pt/GaN contacts. This technique allows us to determine the barrier height with a spatial resolution of about 10–20 nm (i.e., of the order of the tip diameter).[21] In particular, scanning the biased tip over an area of 25 μm^2 (in a 10×10 matrix), a statistic distribution of the local values of the barrier height in different positions of the Pt/GaN interface was determined. The statistical distribution of the barrier height values determined by this procedure are reported in Figs. 6(a) and 6(b) for the as-deposited sample and for the sample annealed at 400 °C, respectively. Clearly, a wide distribution of the barrier height values is found for both samples, thus demonstrating the lateral inhomogeneity of the Schottky barrier on a nanometer scale. Moreover, the fits superimposed with the experimental data indicate that the barrier inhomogeneity is described by a Gaussian distribution of barrier height values. It is important to point out that postdeposition thermal annealing induces a strong modification in the distribution of the barrier height values. In particular, the peak of the histogram (i.e., the average value of Φ_B) increases, whereas the standard deviation significantly decreases upon annealing at 400 °C. For the as-deposited sample, an average value of $\Phi_B = 0.74$ eV and a standard deviation of $\sigma_\Phi = 0.27$ eV were determined by the Gaussian fit of the data. After annealing at 400 °C, the average Schottky barrier Φ_B increases up to 0.84 eV, while the σ_Φ becomes significantly narrower, i.e., 0.11 eV. Since the nanoscale electrical analysis on the bare GaN surface indicated no significant modification upon annealing, this improvement in the Pt/GaN Schottky barrier height distribution can be ascribed to an improvement of the metal/semiconductor interface intrinsic properties (removal of a nonuniform residual processing-induced contaminants, reduction of the interface state density, better metal adhesion, etc.).

C. Role of the nanoscale barrier inhomogeneity on the electrical parameters

The nanoscale local electrical properties of the Schottky barrier were correlated with the temperature dependent electrical behavior of the macroscopic Schottky diodes.

First, it is interesting to point out that the mean value of Φ_B determined by the nanoscale local *I-V* measurements is in good agreement with the value of the barrier height extracted from the forward *I-V* curves of the macroscopic diodes. Furthermore, the narrowing of the barrier height distribution width observed upon annealing at 400 °C is an indication of an improvement of the contact homogeneity, which, in turn, can be associated with the improvement of the ideality factor of the diode. However, even after postdeposition annealing, we are in the presence of a real Schottky barrier, i.e., a distribution of the barrier height values.

Two well consolidated approaches to describe inhomogeneous Schottky barriers are those proposed by Tung[26] and by Werner and Güttler,[33] which assume a Gaussian distribution of the barrier height values on the metal/semiconductor interface. Tung depicts an inhomogeneous contact as a distribution of regions ("patches") with different low barrier height values and areas embedded in a uniform higher Schottky barrier area.[26] Hence, the current through a small patch is influenced by the surrounding area with a higher barrier height, thus resulting in an effective Schottky barrier and an effective area depending on the patch parameter and the bias.[26,34] On the other hand, Werner and Güttler[33] assume a continuous spatial distribution of the barrier, and the total current across a Schottky diode is obtained by integrating the thermionic emission current with an individual barrier height and weighted by using the Gaussian distribution function. This approach, however, does not consider the lateral length scale of the inhomogeneity and the pinch-off effect related to the interaction between adjacent regions with different barriers and obtains that the effective barrier is always lower than the mean value of the barrier distribution. Since the nanoscale measurements demonstrated a Gaussian distribution of the barrier height along the metal/GaN interface, with a mean value (0.84 eV) comparable with the value obtained by the

forward *I-V* curves of the macroscopic diodes, Tung's model results to be more appropriate in describing the barrier inhomogeneity. This assumption is also confirmed by the linear relationship between the barrier height and the ideality factor [Fig. 3(b)].

According to Tung's approach, the potential distribution below the low barrier patches is affected by the "pinch-off" effect of the low barrier regions by the surrounding average uniform high barrier, thus resulting in an effective Schottky barrier height Φ_i^{eff} under the single patch, which is given by the following expression:[34]

$$\Phi_i^{\text{eff}} = \Phi_{B0} - \gamma_i \left(\frac{V_{\text{bb}}}{\eta} \right)^{1/3}, \tag{2}$$

where γ_i is a parameter describing the barrier inhomogeneity and depends both on the patch size and on the deviation of the local barrier Φ_i^{eff} from the ideal higher barrier Φ_{B0}, V_{bb} is the band bending, and $\eta = \varepsilon / qN_D$, with ε being the permittivity of the material, q the electron charge, and N_D the carrier concentration in the semiconductor. The single Φ_i^{eff} values are given by the Schottky barrier obtained through the local *I-V* measurements. On the other hand, the value of $\Phi_{B0}=1.21$ eV is given by the asymptotic extrapolation at $n=1$ ("ideal" case) of the plot of Φ_B as a function of n, shown in Fig. 3(b). Indeed, for an inhomogeneous Schottky contact, a linear relationship between the barrier height and the ideality factor is expected.[25]

Under a macroscopic point of view, the lateral inhomogeneity of the contact results in the so-called T_0 anomaly, i.e., a temperature dependence of the ideality factor as

$$n = 1 + \frac{T_0}{T}, \tag{3}$$

where T_0 is a constant related to the barrier distribution. For a Gaussian distribution of the barrier height values, as that observed experimentally, in our previous work, we have demonstrated that the relation between T_0 and standard deviation σ_Φ of the barrier height distribution is[19]

$$T_0 = \frac{q\sigma_\Phi^2}{3kV_{\text{bb}}}. \tag{4}$$

In particular, a value of $T_0=43$ K is obtained using the standard deviation $\sigma_\Phi=0.11$ eV extracted by the nanoscale measurements for the sample annealed at 400 °C. The parameter T_0 correlates the temperature dependence of the ideality factor and the nanoscale electrical measurements. Figure 7 reports the experimental plot of nkT versus kT, together with the theoretical curve obtained substituting in Eq. (3) the value of $T_0=43$ K determined through the standard deviation of the barrier height distribution. As can be seen, a good agreement between the experimental data and the theoretical model is obtained. Moreover, the dashed line representing the behavior of ideal Schottky contact (with $n=1$) was also reported.

Another experimental evidence that can be explained as a consequence of inhomogeneous nature of Schottky barrier is the temperature behavior of barrier height, shown in Fig. 3(a). In particular, according to Tung's model, the temperature dependence of barrier height in the presence of regions (patches) with lower barrier height values is given by the following relation:

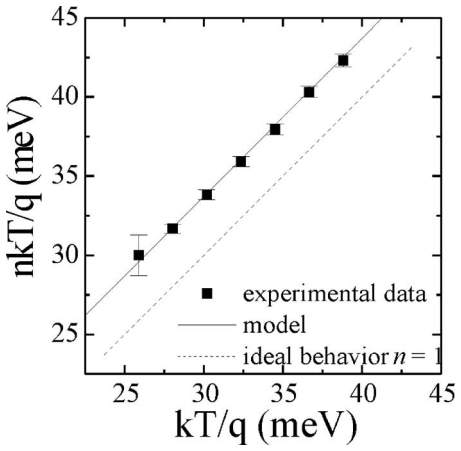

FIG. 7. Plot of nkT as a function of kT and of the theoretical curve obtained from the nanoscale barrier height distribution using $T_0=43$ K. The behavior of ideal Schottky contact (with $n=1$) is also reported (dashed line).

$$\Phi_B(T) = \Phi_{B0} - \beta\kappa V_{\text{bb}}^{2/3}, \tag{5}$$

where σ_γ is the standard deviation of the distribution of the γ_i values, $\beta = q/kT$, and $\kappa = \sigma_\gamma^2 / 2\eta^{2/3}$. Substituting in this relation the value of and using the Eq. (3) of Ref. 19, which relates the standard deviation of $\gamma_i(\sigma_\gamma)$ with that of the barrier height values (σ_Φ),

$$\Phi_B(T) = \Phi_{B0} - \frac{\beta\sigma_\Phi^2}{2}. \tag{6}$$

Hence, the theoretical temperature dependence of barrier height is obtained using the standard deviation σ_Φ extracted by the nanoscale measurements for the sample annealed at 400 °C and $\Phi_{B0}=1.21$ eV. In particular, Fig. 8 reports the experimental data plot of $2\Phi_B/\beta$ versus $2/\beta$ obtained by the *I-V* measurements on macroscopic diodes [Fig. 3(a)] together with the theoretical barrier values extracted by Eq. (6). In this case as well, a good agreement between the experimental and theoretical data is obtained.

Besides the temperature behavior of the barrier height and of the ideality factor, the combination between the mac-

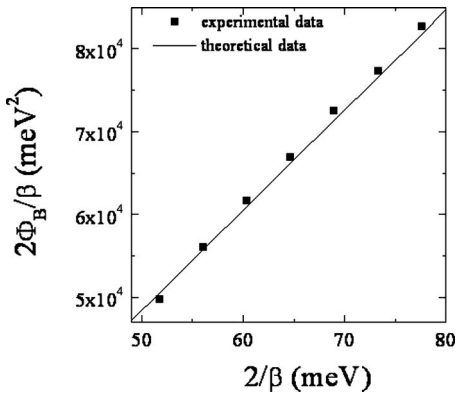

FIG. 8. Plot of $2\Phi_B/\beta$ vs $2/\beta$ with experimental data and the theoretical barrier values extracted by Eq. (6).

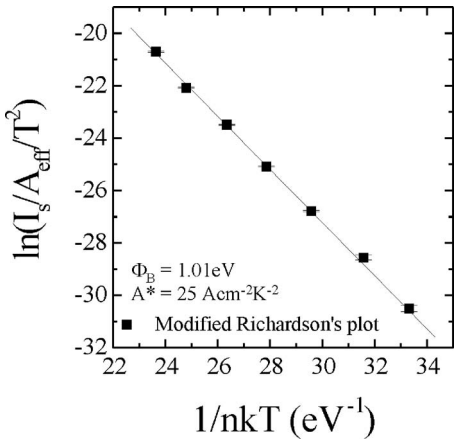

FIG. 9. Modified Richardson plot $\ln(I_s/A_{\text{eff}}T^2)$ vs $1/nk_BT$ of the sample annealed at 400 °C.

roscopic and the nanoscale electrical characterization of the inhomogeneous Pt/GaN Schottky barrier allowed us to explain the experimental low values of the Richardson's constant A^*.

Assuming a statistical distribution of the patches with different areas and characterized by effective barrier heights, the total current flowing through the metal/semiconductor contact is approximately given by this phenomenological relation[35]

$$I_{\text{total}} = A_{\text{eff}}A^*T^2\left[\exp\left(\frac{qV}{k(T+T_0)}\right)-1\right]\exp\left(-\frac{q\Phi_B(T)}{k(T+T_0)}\right), \tag{7}$$

where A_{eff} is the effective area of Schottky contact, taking into account that the area involved in the current flow in a nonuniform metal/semiconductor can only be a fraction of the geometric contact area.

The experimental *I-V-T* curves of the sample annealed at 400 °C were fitted with this equation, where the values of $\Phi_B(T)$ were determined by Eq. (6), and the value of T_0 was extracted by Eq. (4), using for both the standard deviation of barrier heights distribution obtained by the nanoscale measurements. In this way, the values of the effective area A_{eff} at different temperatures, were obtained. As an example, at room temperature a value of 1.5×10^{-5} cm^2 is obtained, thus indicating that the effective area involved in the current transport is significantly lower (i.e., only 2%) of the entire geometric area of the Schottky contact. Therefore, the Richardson's plot was modified using the temperature dependent values of A_{eff}. Figure 9 shows the Richardson's plot modified using the different values of A_{eff} at the different temperatures, i.e., $\ln(I_s/A_{\text{eff}}T^2)$ versus $1/nk_BT$. From the slope and the intercept of the linear fit, an effective barrier height of 1.01 eV and a value of the Richardson's constant of 25 ± 9 A cm^{-2} K^{-2} were obtained. Interestingly, the value of A^* is in reasonable agreement with the theoretical value of 26.9 A cm^{-2} K^{-2}. Therefore, the commonly observed underestimation of the Richardson's constant in GaN can be attributed to the Schottky barrier inhomogeneity that, in turn, translates itself into an effective area interested by the current transport lower than the geometric area of the contact. In particular, as demonstrated by the nanoscale analysis of the bare GaN surface, the inhomogeneous current transport, caused by the presence of preferential conductive current paths in the proximity of material surface defects, is one of the physical causes of the reduction of the effective area and hence of the anomalous behavior of the electrical parameters. On the basis of the nanoscale analysis of the bare GaN surface, it is possible to roughly estimate the effects of the material defects, such as dislocations reaching the surface, on the electrical parameters of the Pt/GaN contacts. As determined by morphological analysis on the GaN surface, considering a dislocation density of about $\sim5\times10^8$ cm^{-2}, it can be estimated that $(3-4)\times10^{-5}$ are present in the area of the macroscopic diode. Hence, basing on the SCM results, assuming an on average diameter of 100 nm, the area covered by the preferential conductive path is 2.78×10^{-5} cm^2, i.e., around 4% of the geometric area of the diode. Hence, it is not surprising that the effective area determined by the analytical description of the barrier inhomogeneity is in the order of 2% of the entire geometric area of the contact.

Furthermore, the improvement of the barrier homogeneity observed after postdeposition annealing cannot be related to the material defects, since the nanoscale analysis of the sample surface did not show any change upon annealing at this temperature. Plausibly, the higher degree of homogeneity (better ideality factor, narrower barrier height distribution) is associated with an improvement of the intimate properties of the metal/semiconductor interface after annealing. As an example, it cannot be ruled out that the improvement of the barrier properties upon annealing can be ultimately associated with a reduction of the interface state density.[6]

IV. CONCLUSION

The temperature dependence of the electrical properties of Pt/GaN Schottky barrier was investigated in the range of 25–175 °C. From the measurements on macroscopic Schottky diodes, a temperature dependence of the barrier height and of the ideality factor was observed. This behavior was clarified through a nanoscale electrical characterization of the Schottky contact, demonstrating the presence of a lateral inhomogeneity of the Schottky barrier, and discussed in terms of Tung's model. Besides the temperature behavior of the barrier height and of the ideality factor, the inhomogeneous nature of the Pt/GaN Schottky barrier allowed us to explain the experimental low values of the Richardson's constant A^*. Indeed, the correct value of the Richardson's constant was obtained using a modified Richardson's plot, which considers the temperature dependence of an effective area lower than the total area of the diode. Nanoscale electrical characterization performed on the bare sample surface demonstrated that the reduction of the effective area interested by the current transport is strongly related to the material quality.

ACKNOWLEDGMENTS

The authors thank S. Di Franco for his support during device fabrication. This work was supported by ST Microelectronics Catania and by FIRB Project No.

RBIP068LNE_001 of the Italian Minister for Research.

[1]S. Nakamura, T. Mukai, and M. Senoh, Appl. Phys. Lett. **64**, 1687 (1994).
[2]A. Zhang, F. Ren, J. Han, S. Pearton, S. S. Park, Y. J. Park, and J. Chyi, in *Wide Energy Bandgap Electronic Devices*, edited by F. Ren and J. C. Zolper (World Scientific, Singapore, 2003).
[3]*Gallium Nitride Processing for Electronics, Sensors and Spintronics*, edited by S. J. Pearton, C. R. Abernathy, and F. Ren (Springer-Verlag, London, 2006).
[4]E. H. Rhoderick and R. H. Williams, *Metal-Semiconductor Contacts* (Clarendon, Oxford, 1988).
[5]L. Wang, M. I. Nathan, T.-H. Khan, and Q. Chen, Appl. Phys. Lett. **68**, 1267 (1995).
[6]N. Miura, T. Oishi, T. Nanjo, M. Suita, Y. Abe, T. Ozeki, H. Ishikawa, and T. Egawa, IEEE Trans. Electron Devices **51**, 297 (2004).
[7]J. Xie, Y. Fu, X. Ni, S. Chevtchenko, and H. Morkoç, Appl. Phys. Lett. **89**, 152108 (2006).
[8]Q. Z. Liu and S. S. Lau, Solid-State Electron. **42**, 677 (1998).
[9]Y.-J. Lin, Q. Ker, C.-Y. Ho, H.-C. Chang, and F.-T. Chien, J. Appl. Phys. **94**, 1819 (2003), and references therein.
[10]M. L. Lee, J. K. Sheu, and S. W. Lin, Appl. Phys. Lett. **88**, 032103 (2006).
[11]M. Missous and E. H. Rhoderick, J. Appl. Phys. **69**, 7142 (1991).
[12]F. Roccaforte, F. La Via, V. Raineri, R. Pierobon, and E. Zanoni, J. Appl. Phys. **93**, 9137 (2003).
[13]P. Hacke, T. Detchprohm, K. Hiramatsu, and N. Sawaki, Appl. Phys. Lett. **63**, 2676 (1993).
[14]J. D. Guo, F. M. Pan, M. S. Feng, R. J. Guo, P. F. Chou, and C. Y. Chang, J. Appl. Phys. **80**, 1623 (1996).
[15]L. S. Yu, Q. Z. Liu, Q. J. Xing, D. J. Qiao, S. S. Lau, and J. Redwing, J. Appl. Phys. **84**, 2099 (1998).
[16]E. J. Miller, D. M. Schaadt, T. Yu, X. L. Sun, L. J. Brillson, P. Waltereit, and J. S. Speck, J. Appl. Phys. **94**, 7611 (2003).
[17]E. G. Brazel, M. A. Chin, and V. Narayanamurti, Appl. Phys. Lett. **74**, 2367 (1999).
[18]F. Roccaforte, F. Iucolano, F. Giannazzo, A. Alberti, and V. Raineri, Appl. Phys. Lett. **89**, 022103 (2006).
[19]F. Iucolano, F. Roccaforte, F. Giannazzo, and V. Raineri, Appl. Phys. Lett. **90**, 092119 (2007).
[20]F. Iucolano, F. Roccaforte, A. Alberti, C. Bongiorno, S. Di Franco, and V. Raineri, J. Appl. Phys. **100**, 123706 (2006).
[21]F. Giannazzo, F. Roccaforte, V. Raineri, and S. F. Lotta, Europhys. Lett. **74**, 686 (2006).
[22]A. M. Witowski, K. Pakuła, J. M. Baranowski, M. L. Sadowski, and P. Wyder, Appl. Phys. Lett. **75**, 4154 (1999).
[23]K. J. Duxstad, E. E. Haller, and K. M. Yu, J. Appl. Phys. **81**, 3134 (1997).
[24]Q. Z. Liu, L. S. Yu, S. S. Lau, J. M. Redwing, N. R. Perkins, and T. F. Kuech, Appl. Phys. Lett. **70**, 1275 (1997).
[25]R. F. Schmitsdorf, T. U. Kampen, and W. Mönch, J. Vac. Sci. Technol. B **15**, 1221 (1997).
[26]R. T. Tung, Mater. Sci. Eng., R. **35**, 1 (2001).
[27]R. Hackam and P. Harrop, IEEE Trans. Electron Devices **19**, 1231 (1972).
[28]Y. Zhou, D. Wang, C. Ahyi, C.-C. Tin, J. Williams, M. Park, N. M. Williams, A. Hanser, and E. A. Preble, J. Appl. Phys. **101**, 024506 (2007).
[29]H. Ishikawa, K. Nakamura, T. Egawa, T. Jimbo, and M. Umeno, Jpn. J. Appl. Phys., Part 2 **37**, L7 (1998).
[30]A. R. Arehart, B. Moran, J. S. Speck, U. K. Mishra, S. P. DenBaars, and S. A. Ringel, J. Appl. Phys. **100**, 023709 (2006).
[31]F. Iucolano, F. Giannazzo, F. Roccaforte, L. Romano, M. G. Grimaldi, and V. Raineri, Nucl. Instrum. Methods Phys. Res. B **257**, 336 (2007).
[32]P. J. Hansen, Y. E. Strausser, A. N. Erickson, E. J. Tarsa, P. Kozodoy, E. G. Brazel, J. P. Ibbetson, U. Mishra, V. Narayanamurti, S. P. DenBaars, and J. S. Speck, Appl. Phys. Lett. **72**, 2247 (1998).
[33]J. H. Werner and H. H. Güttler, J. Appl. Phys. **69**, 1522 (1991).
[34]J. Sullivan, R. T. Tung, M. Pinto, and W. R. Graham, J. Appl. Phys. **70**, 7403 (1991).
[35]R. T. Tung, Phys. Rev. B **45**, 13509 (1992).